ISSN 1 746-7233, England, UK
World Journal of Modelling and Simulation
Vol. 12 (2016) No. 4, pp. 281-291

Design methodology for torque-angle control of a non-linear vector controlled permanent magnet synchronous motor

Pilla Ramana[1]*, Karlapudy Alice Mary[2], Munagala Surya Kalavathi[3]

[1] Dept. of EEE, GMR Institute of Technology, Rajam, AP-532127, India
[2] Vignan's Institute of Information Technology, Visakhapatnam, AP-533045, India
[3] Dept. of EEE, JNTUH College of Engineering, JNTUH, Hyderabad, Telangana-500085, India

(*Received June 15 2015, Accepted June 1 2016*)

Abstract. Synchronous motor drives are emerging as an attractive alternative to DC and Induction Motor drives, especially in high power, low speed range. Different types of control schemes have been suggested for variable speed AC drives fed from static power converters. Among them direct and indirect vector control strategies have become quite popular in recent years. When applied the above scheme to synchronous motor drives, there are certain drawbacks like instability or abrupt stopping due to some constraints. In this work, to overcome the above drawbacks, a generalized design strategy is suggested for speed control loop of an inverter fed Permanent Magnet Synchronous Motor (PMSM) drive; in which its inherent flexibility to generate the same torque for different combinations of currents is exploited. The closed loop system for an inverter fed PMSM drive is simulated using MATLAB/SIMULINK. The performance figures of torque angle control as well as field oriented control can be obtained and verified through simulation for different power factors of the motor ranging from lagging to leading through unity.

Keywords: permanent magnet synchronous motor, field oriented control, unity power factor control, torque angle control

1 Introduction

The Permanent Magnet Synchronous Motor (PMSM) is similar to the salient pole motor, except that there is no field winding and the field is provided instead by mounting permanent magnets in the rotor. The excitation voltage cannot be varied. The elimination of field coil, dc supply and slip rings reduces the motor losses and complexity and hence improves the efficiency and p.f. So these motors are finding increasing applications in robots, electrical vehicles and machine tools. Over the years different methods of closed loop control have been envisaged for improving the stability and dynamic response of the variable speed PMSM drives[8, 9] fed from static devices either in open loop mode or in self-control mode involving stator voltage or current control[4], torque angle control[11], power factor control[13] and field oriented control[10, 12].

When driving a synchronous machine directly from the mains, the flux and torque will arise automatically in relation to the load[1], which leads to the variation of torque angle. The torque angle (δ) is defined as the angle between terminal voltage and excitation voltage, and also called as load angle or power angle. The load leads to a modification of the torque angle until the steady state is reached. The transition occurs in the form of a periodic oscillation, which must be attenuated with damper windings. The variation of the torque angle δ complies with rotating the applied stator flux in relation to the rotor position without variation of the magnitude of the stator voltage. As long as the synchronous machine is in the stable region, the relation between torque angle and torque is proportional, so the torque angle can be utilized to control the torque. If the load on the

* Corresponding author. *E-mail address*: pramana.gmrit@gmail.com, ramana.pilla@gmrit.org.

motor increases, the rotor initially slows down, this increases torque angle δ. As a result, the induced torque increases, speeding up the rotor up to the synchronous speed with a larger torque angle.

Control system design for inverter-fed drives used the classical transfer function approach for single-input single-output (SISO) systems, proportional plus integral (PI) controllers were designed for individual control loops[7]. It is found that the transient response of a PI controller is slow and is improved by pole placement through state feedback. However, the effective gains of the PI controller are substantially decreased as a function of the increase of motor speed. Hence, the transient response is fast, another advantage of the scheme is that the modulation scheme utilizes space voltage vector PWM which gives a wider linear control voltage range than the ramp comparison method[3]. However, since the predictive controller does not have an integral control, a steady state error may exist, if the motor modeling is inexact or the motor parameters vary under operation.

The proposed controller is represented in the conventional two-loop structure for the motor drive as shown in Fig. 1. The two loops are named as one is outer speed loop and second one is inner current loop. The outer loop has the speed controller, the output of which is the reference value of the torque, T_e^* from this value, the reference values of the currents i.e., i_{qs}^* and i_{ds}^* are computed for a desired internal angle (ψ) and desired torque angle (δ). This gives flexibility in choosing the power factor of the motor from lagging to leading values including unity. The field oriented control can also be obtained as a special case, by setting the power factor angle to be equal to the torque angle, resulting in complete decoupling between the armature flux and the field flux, thus producing a DC motor like behavior. In this sense, the proposed control scheme is more general than conventional field oriented control.

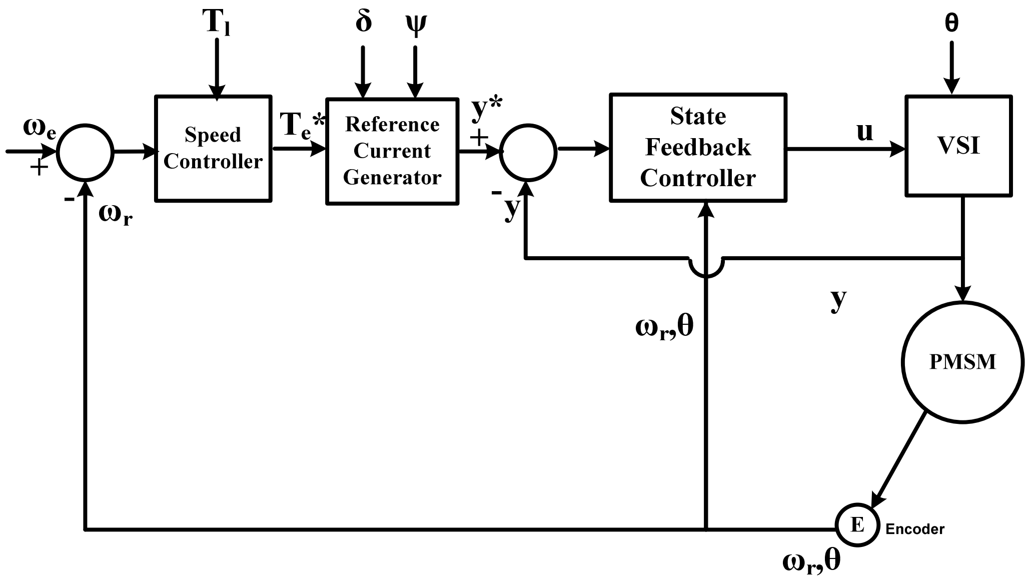

Fig. 1: Block diagram representation of the proposed control scheme

This paper is organized as follows: Firstly the mathematical model of PMSM is derived in section 2. Then the design of speed controller is given section 3 and the reference current generation for desired torque angle, δ is given in section 4. The state feedback controller design is given in section 5 and design guidelines are given in section 6. The simulation results are presented and discussed in section 7. Finally the concluding remarks are presented in section 8.

2 Modeling of permanent magnet synchronous motor

The design of the control system for a high performance drive requires a mathematical model of the motor. This is usually derived from the physical principles[6]. Then, the parameters of the motor are determined through off-line testing or estimated on-line from the input/output operating records. The schematic diagram of PMSM with damper windings is as shown in Fig. 2. The model of PMSM has been developed on rotor reference frame[5] using the following assumptions:

- Saturation is neglected.
- Space harmonics in the air-gap are neglected.
- Air-gap reluctance has a constant component as well as a sinusoidal varying component.
- The induced e.m.f. is sinusoidal.
- Eddy currents and hysteresis losses are negligible.

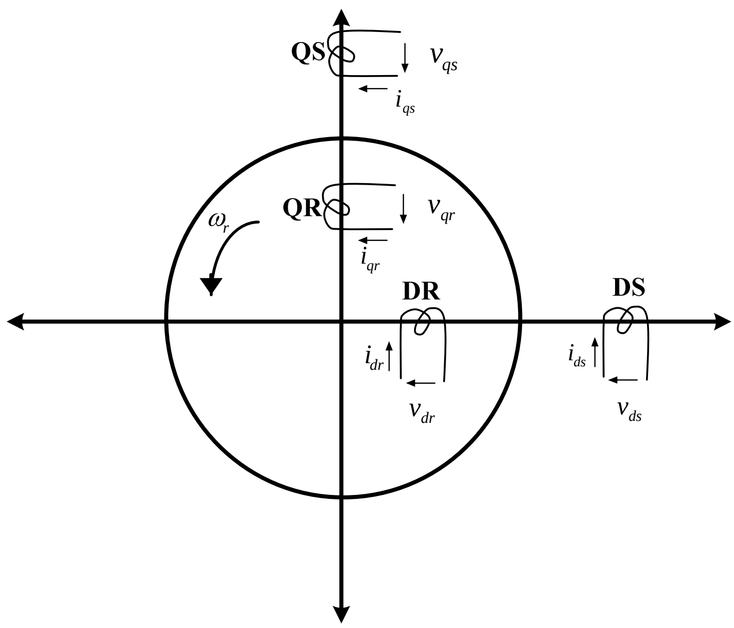

Fig. 2: Schematic diagram of PMSM with damper windings

The voltage equations of PMSM in rotor reference frame are

$$v_{qs} = r_a i_{qs} + l_{qs} p i_{qs} + l_{aq} p i_{qr} + \omega_r l_{ds} i_{ds} + \omega_r l_{ad} i_{dr} + \omega_r \Psi, \tag{1}$$

$$v_{ds} = r_a i_{ds} + l_{ds} p i_{ds} + l_{ad} p i_{dr} - \omega_r l_{qs} i_{qs} - \omega_r l_{aq}, \tag{2}$$

$$v_{qr} = r_{qr} i_{qr} + l_{qr} p i_{qr} + l_{aq} p i_{qs}, \tag{3}$$

$$v_{dr} = r_{dr} i_{dr} + l_{dr} p i_{dr} + l_{ad} p i_{ds}, \tag{4}$$

where, $\Psi = l_{ad} i_{fr} =$ air gap flux linkage

The Eq. (1) can be rewritten as

$$v'_{qs} = (v_{qs} - \omega_r \Psi) = r_a i_{qs} + l_{qs} p i_{qs} + l_{aq} p i_{qr} + \omega_r l_{ds} i_{ds}. + \omega_r l_{ad} i_{dr} \tag{5}$$

The electrical torque developed is

$$T_e = \frac{3}{2}\frac{P}{2}[(l_{ad} - l_{aq}) i_{qs} i_{ds} + l_{ad} i_{qs} i_{dr} - l_{aq} i_{qr} i_{ds} + \psi i_{qs}]. \tag{6}$$

The torque balance equation is

$$\frac{2}{P} J p \omega_r = T_e - T_l - \frac{2}{P} \beta \omega_r, \tag{7}$$

where the subscripts q_s, d_s, q_r and dr correspond to q and d axis quantities for the stator(s) and rotor(r) in all combinations, r_a denotes the armature resistance, l_{qs} denotes quadrature axis inductance, l_{ds} denotes direct axis inductance etc. and T_e is the developed torque. The rotor speed is given by ω_r and the load torque by T_l. J is moment of inertia, P is the number of poles and β is the co-efficient of viscous friction. The derivative operator is represented by the symbol p.

Representing the voltage Eq. (1), (2), (3), (5) into a state space form is as given below:

$$\begin{bmatrix} v'_{qs} \\ v_{ds} \\ v_{qr} \\ v_{dr} \end{bmatrix} = \begin{bmatrix} r_a & \omega_r l_{ds} & 0 & \omega_r l_{ad} \\ -\omega_r l_{qs} & r_a & -\omega_r l_{aq} & 0 \\ 0 & 0 & r_{qr} & 0 \\ 0 & 0 & 0 & r_{dr} \end{bmatrix} \cdot \begin{bmatrix} i_{qs} \\ i_{ds} \\ i_{qr} \\ i_{dr} \end{bmatrix} + \begin{bmatrix} l_{qs} & 0 & l_{aq} & 0 \\ 0 & l_{ds} & 0 & l_{ad} \\ l_{aq} & 0 & l_{qr} & 0 \\ 0 & l_{ad} & 0 & l_{dr} \end{bmatrix} \cdot \begin{bmatrix} pi_{qs} \\ pi_{ds} \\ pi_{qr} \\ pi_{dr} \end{bmatrix}. \quad (8)$$

Hence by using system and torque equations one can model Permanent Magnet Synchronous motor.

3 Design of the speed controller

In the conventional two-loop structure as shown in Fig. 1, a proportional plus integral (PI) controller is used as a speed controller[14] in the outer loop. The output of the PI controller is the reference torque T_e, from which the reference currents, i^*_{qs} and i^*_{ds} can be generated. The design of the gain constants of this controller is as follows:

The torque balance Eq. (7) for no. of poles, $P = 4$ is taken as

$$p\omega_r = \frac{2}{J}[T_e - T_l - \frac{\beta\omega_r}{2}], \quad (9)$$

The equation of PI controller is

$$T^*_e = k_p e + k_i \int_0^t e dt, \quad (10)$$

where,

$$e = (\omega_e - \omega_r). \quad (11)$$

Here ω_s is the set speed, ω_r is the reference speed and k_p and k_i are the proportional and integral gains of the PI controller respectively. On substituting Eq. (10), (11) in Eq. (9) and taking Laplace transform,

$$(s\omega_r - \omega_{r0}) = \frac{2}{J}\left[\left(k_p + \frac{k_i}{s}\right)(\omega_e - \omega_r) - T_l - \left(\frac{\beta}{2}\right)\omega_r\right]. \quad (12)$$

For $T_l = 0$ and $\omega_{r0} = \omega_e$ rearranging the terms in Eq. (12), from which the ratio, $\frac{\omega_r}{\omega_e}$ is obtained as

$$\frac{\omega_r}{\omega_e} = \frac{\frac{2}{j}\left(k_p + \frac{k_i}{s}\right) + 1}{s + \frac{\beta}{J} + \frac{2}{J}\left(k_p + \frac{k_i}{s}\right)} = \frac{\left(k_p + \frac{k_i}{s}\right)s + \frac{2}{J}k_i}{s^2 + \left(\frac{\beta}{J} + \frac{2}{J}k_p\right)s + \frac{2}{J}k_i}. \quad (13)$$

This is the standard form of transfer function for a second order system and the denominator can be represented in the form

$$s^2 + 2\zeta\omega_n s + \omega_n^2 = 0. \quad (14)$$

The characteristics of the above system is

$$s^2 + \left(\frac{\beta}{J} + \frac{2}{J}k_p\right)s + \frac{2}{J}k_i = 0. \quad (15)$$

Therefore, equating the corresponding terms in Eqs. (14) and (15)

$$\omega_n^2 = \frac{2k_i}{J}, \tag{16}$$

$$2\zeta\omega_n = \frac{\beta}{2} + \frac{2k_p}{J}. \tag{17}$$

From the above Eqs. (16) and (17), the controller gains, k_i and k_p are obtained as,

$$k_i = \frac{J}{2}\omega_n^2, \tag{18}$$

$$k_p = J\zeta\omega_n - \frac{\beta}{2}. \tag{19}$$

Assigning proper values of ζ and ω_n and using the values of J and β, the numerical values of k_p and k_i can be computed.

4 Determination of reference currents

The developed electrical torque in Eq. (6) is a function of the states i.e., the stator and rotor (field and damper) currents of the PMSM. Since, this function is a non-linear; there are many possible values of these currents for the generation of the same torque. Thus, there is a great deal of flexibility in the choice of the reference values for these currents. The following three conditions are imposed to obtain unique solutions for these reference currents

(a) The arbitrary setting of internal angle, ψ.
(b) The arbitrary setting of torque angle, δ
(c) All the reference currents should be real valued.

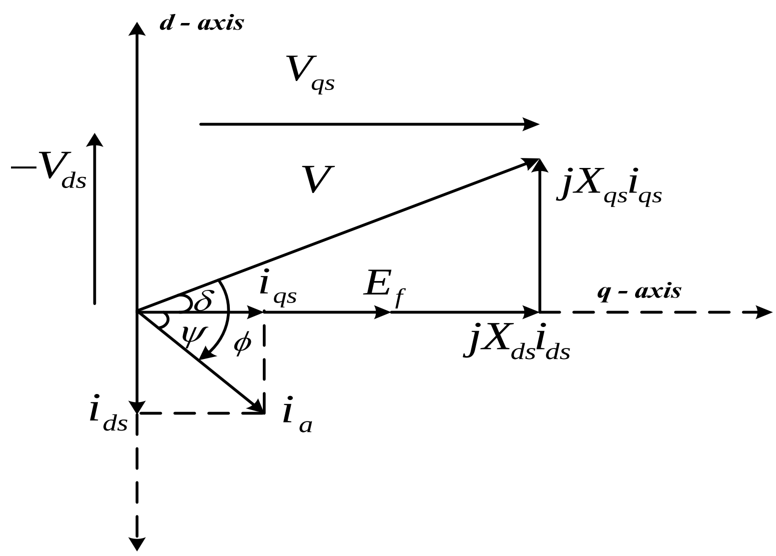

Fig. 3: Phasor diagram

The phasor diagram of a PMSM is as shown in Fig. 3. Referring to the phasor diagram

$$\tan\delta = \frac{-v_{ds}}{v_{qs}}. \tag{20}$$

Substituting v_{qs} and v_{ds} values in Eq. (20)

$$\tan\delta = \frac{-r_a i_{ds} - l_{ds} p i_{ds} - l_{ad} p i_{ds} + \omega_r l_{qs} i_{qs} + \omega_r i_{aq} i_{qr}}{r_a i_{qs} + l_{qs} p i_{qs} + l_{aq} p i_{qr} + \omega_r l_{ds} i_{ds} + \omega_r l_{ad} i_{dr} + \omega_r \Psi}. \tag{21}$$

Under steady state condition with all p or $\frac{d}{dt}$ terms as well as i_{dr} and i_{qr} assumed to be zero. Then the above equation can be written as

$$\tan\delta = \frac{\omega_r l_{qs} i_{qs} - r_a i_{ds}}{r_a i_{qs} + \omega_r l_{ds} i_{ds} + \omega_r \Psi}. \tag{22}$$

Also,

$$i_{ds} = i_{qs}\tan\psi. \tag{23}$$

With a permanent magnet on the rotor, the motor has a constant flux linkage, Ψ. Three sets of formulae for the reference currents are derived-one with specified δ, second with specified ψ and the third for field oriented (FO) case. Here in this section, the one with specified δ is considered and the rest is considered elsewhere.

Taking Torque angle, δ as a specification:

From Eq. (22)

$$(r_a \tan\delta - \omega_r l_{qs}) i_{qs} = i_{ds}(-\omega_r l_{ds}\tan\delta - r_a) - \omega_r \Psi \tan\delta. \tag{24}$$

Also the steady state torque from the above equation for number of poles, $P = 4$

$$\begin{aligned} T_e &= 3[(l_{ad} - l_{aq}) i_{ds} i_{qs} + \Psi i_{qs}], \\ i_{qs} &= \frac{T_e}{3\left[(l_{ad} - l_{aq}) i_{ds} + \Psi\right]}. \end{aligned} \tag{25}$$

From Eqs. (24) and (25)

$$(r_a \tan\delta - \omega_r l_{qs}) \left[\frac{T_e}{3\left[(l_{ad} - l_{aq}) i_{ds} + \Psi\right]}\right] = i_{ds}(-\omega_r l_{ds}\tan\delta - r_a) - \omega_r \Psi \tan\delta. \tag{26}$$

After simplifying the above equation

$$i^*_{ds} = \frac{-q_2 \pm \sqrt{q_2^2 - 4q_1 q_3}}{2q_1}. \tag{27}$$

where

$$\begin{aligned} q_1 &= 3(l_{ad} - l_{aq})(-r_a - \omega_r l_{ds}\tan\delta), \\ q_2 &= -3(l_{ad} - l_{aq})\omega_r \Psi \tan\delta + 3\Psi(-r_a - \omega_r l_{ds}\tan\delta), \\ q_3 &= -3\Psi^2 \omega_r \tan\delta - (r_a \tan\delta - \omega_r l_{qs}) T^*_e. \end{aligned}$$

The value of i^*_{qs} is obtained by substituting the value of i^*_{ds} from Eq. (27) in Eq. (25) as

$$i^*_{qs} = \frac{T^*_e}{3(l_{ad} - l_{aq}) i_{ds} + \Psi}. \tag{28}$$

The dynamic performance of the drive could be improved by varying the torque angle δ within a particular range.

5 State feedback controller

For the regulator model of given multivariable system, the linear feedback control[2] law is applied with a gain matrix of K. In addition, to have complete control over the system dynamics a pole placement technique is used. In this, the poles or eigen values of closed loop system are placed at the desired locations in negative half of the s-plane. Now partitioning K into K_{bs} and K_{is}, multiplied with the regulator model, the control signal $'u'$ in terms of state vector and the integral of the differences of output and reference vectors is given as

$$\dot{u} = Kz = \begin{bmatrix} K_{bs} & K_{is} \end{bmatrix} \begin{bmatrix} \dot{x} \\ y - y_r \end{bmatrix}. \tag{29}$$

Integrating and simplifying, the control law come out as

$$u = K_{bs}x + K_{is} \int_0^t (y - y_r)dt. \tag{30}$$

From the above equation, it is concluded that the integral of output error (IOE) feedback makes the controller as robust from the modeling imperfections and step like disturbances.

6 Design guidelines

The design methodology for the speed controller as outlined in the Section 4 allows one to choose δ independently in order to meet a certain control objective; such as unity power factor, field orientation etc. But, there is scope for more general types of control, which can have useful engineering implications. In this section, the above design specifications are, therefore, being viewed from this perspective.

Conventional synchronous motor in general, is a doubly excited machine, its armature winding is energized from an inverter and its field winding from a DC source. When synchronous motor is working at constant applied voltage, the resultant air gap flux as demanded by constant terminal voltage remains substantially constant. This resultant air gap flux is established by the cooperation of both AC in the armature winding and DC in the field winding. If the field current is sufficient enough to set up the air gap flux, as demanded by constant applied voltage V then magnetizing current or lagging reactive volt ampere required from the AC source is zero and therefore, the motor operates at unity power factor. This field current which causes unity power factor operation of the synchronous motor is called normal excitation or normal field current.

If the field excitation, E_f is made less than the normal excitation i.e. the motor is under excited, then the deficiency in the flux ($=$ constant air gap flux-flux setup by DC in the field winding) must be make-up by the armature winding. In order to do the needful, the armature winding draws a magnetizing current or lagging reactive volt ampere from the AC source and as a result of it, the motor operates at a lagging power factor. In case the field is made more than its normal excitation, i.e. the motor is over excited, then the excess flux ($=$ flux setup by dc in the field winding-resultant air gap flux) must be neutralized by the armature winding. The armature can do so only if it draws a demagnetizing component of current from the AC source. Since in a motor, the magnetizing current lags the applied voltage by about $90°$, the demagnetizing component of current must lead the applied voltage by about $90°$. In view of this, the excess flux can be counter balanced only if the armature takes a demagnetizing current or leading Reactive Volt Ampere from the AC source; consequently the synchronous motor operates at a leading power factor. A laboratory scale PMSM with a damper winding is taken up as case study. The ratings of the machine as well as the values of the parameters are given in the Appendix.

The equations for i_{qs}^* and i_{ds}^* (as derived in section 4) taking δ as specifications are given as

$$i_{qs}^* = \frac{T_e^*}{3(l_{ad} - l_{aq})i_{ds} + \Psi}, \tag{31}$$

$$i_{ds}^* = \frac{-q_2 \pm \sqrt{q_2^2 - 4q_1q_3}}{2q_1}. \tag{32}$$

From the above Eqs. (31) and (32), the armature current per phase is given as

$$i_{a,phase} = \sqrt{(i_{qs}^*)^2 + (i_{ds}^*)^2}. \tag{33}$$

The PMSM with a constant flux corresponding to i_{fr} as 1A is considered. Then for different values of T_e, we can obtain the characteristics of i_{qs}, i_{ds}, armature current and power factor angle as a function of δ as shown in Fig. 4. From these characteristics, the r.m.s currents per phase as well as the power factor for given values of δ and T_e are computed, verified and validated through simulation results. Then found the wide range of practical working values of currents and the power factor for the stable performance of the motor.

For a motor the reactive power, Q is given by

$$Q = \frac{V}{X_s}(V - E_f \cos\delta). \tag{34}$$

Also, from the phasor diagram

$$\delta + \psi = \phi. \tag{35}$$

7 Results and discussions

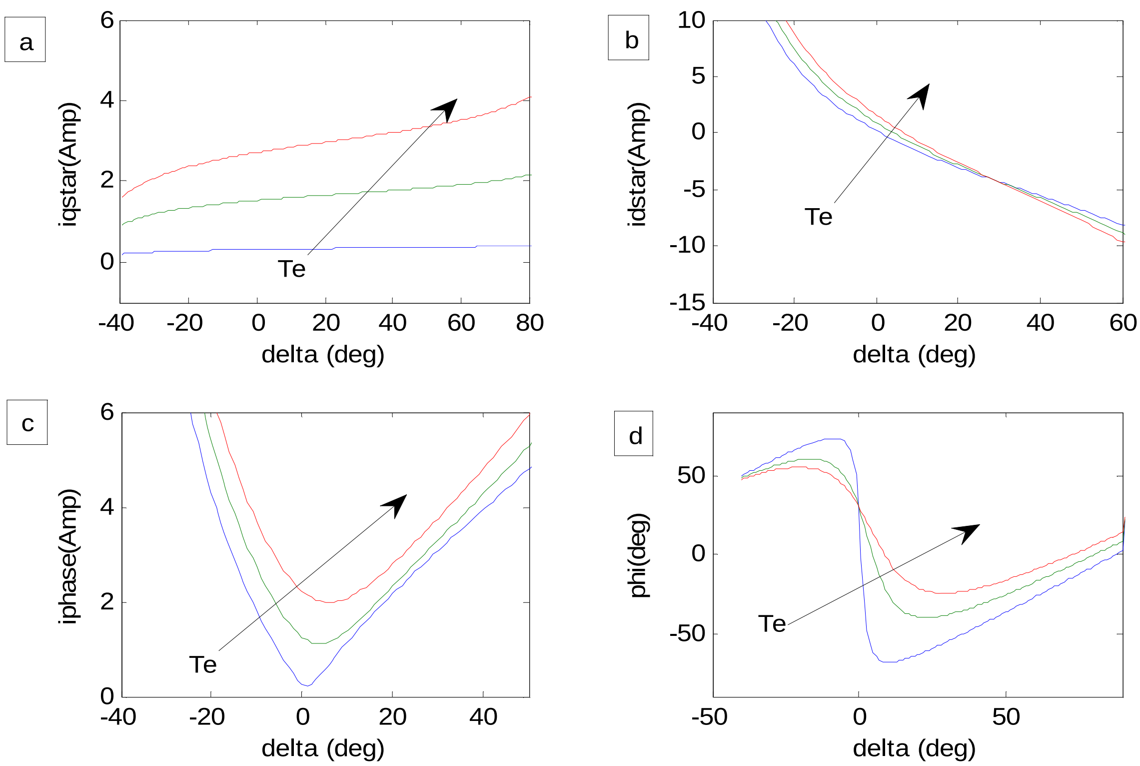

Fig. 4: Family of characteristics of armature currents and power factor angle as a function of δ for different values of T_e

From the above Fig. 4 and Tab. 1, it is concluded that the u.p.f occurs at $\delta = 8.735°$ for the specification of δ with variable T_e. This point indicates $E_f \cos\delta = V$ i.e. normal excitation, under this condition $Q = 0$. For values of δ increasing from 3.8° to 8.735°, $\cos\delta$ decreases, therefore $E_f \cos\delta < V$. It depicts that the motor absorbing reactive power from the supply mains and is operating at a lagging p.f. At the same time ψ achieves positive value and p.f angle ϕ is also positive which is equal to 17°; indicating a lagging p.f. The

Table 1: Performance figures for PMSM as a function of δ for variable T_e (D = design guidelines, S = simulation results)

Design specification	Achieved values of									
δ	ψ through	ϕ through		$\cos\phi$	i_{qs}		i_{ds}		i_{phase}	
Set value	S	D	S	S	D	S	D	S	D	S
3.8 (max. lag)	13.23	17	17.03	-0.25	2.76	2.83	0.65	0.66	2.83	2.90
8.04 (FOC) (lag case)	0.00	8.04	8.04	-0.18	2.82	3.23	0.00	0.00	2.82	3.23
8.23 (min. lag)	-6.63	1.56	1.59	-0.02	2.82	2.88	-0.33	-0.33	2.84	2.89
8.735 (upf value)	-8.734	0.03	0.03	1.0	2.83	2.89	-0.43	-0.44	2.86	2.92
8.74 (min. lead)	-8.75	-0.04	-0.01	0.99	2.83	2.89	-0.44	-0.44	2.86	2.92
35 (max. lead)	-58.63	-23.7	-23.62	0.06	3.15	3.21	-5.17	-5.27	6.05	6.17

field oriented control ($\Psi = 0°$), is achieved at $\delta = \phi = 8.04°$ and the p.f is -0.185 and is found to be always lagging. For values of δ decreasing from $35°$ to $8.735°$, $\cos\delta$ increases. Therefore, $E_f \cos\delta > V$, indicates an over-excited condition, where the reactive power Q is negative, that means motor is delivering reactive power to the mains and hence works at leading p.f. Finally the working range of motor is restricted only from $\delta = 3.8°$ to $35°$ from the simulation even though the range of $\delta = 0°$ to $91°$ in design guidelines.

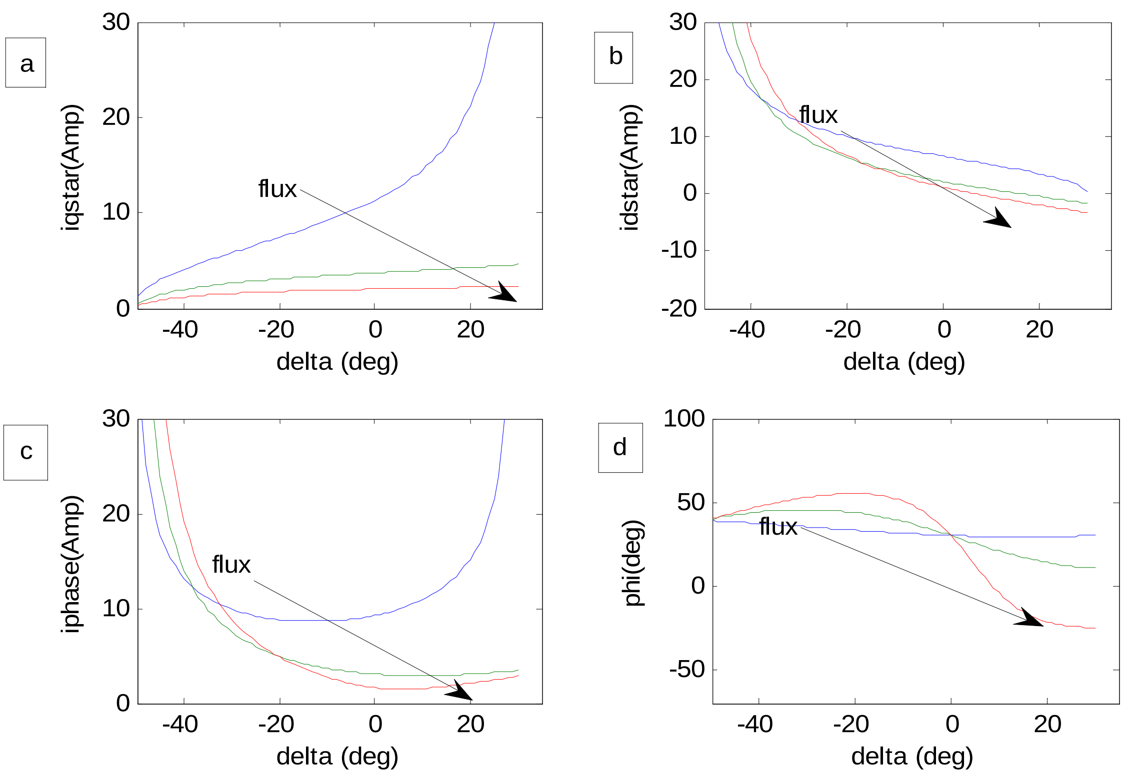

Fig. 5: Family of characteristics of armature currents and power factor angle as a function of for different values of flux

From the above Fig. 5 and Tab. 2, it is concluded that the u.p.f occurs at $\delta = 8.67°$ for the specification of δ with variable flux. This point indicates $E_f \cos\delta = V$ i.e. normal excitation, under this condition $Q = 0$. For values of δ increasing from $-8.0°$ to $8.67°$, $\cos\delta$ decreases, therefore $E_f \cos\delta < V$. It depicts that the motor absorbing reactive power from the supply mains and is operating at a lagging p.f. The field oriented control ($\psi = 0°$), is achieved at $\delta = \phi = 6.67°$ and the p.f is -0.95 and is found to be always lagging. For values of δ decreasing from $30°$ to $8.67°$, $\cos\delta$ increases. Therefore, $E_f \cos\delta > V$, indicates an over-excited condition, where the reactive power Q is negative, that means motor is delivering reactive power to the mains

Table 2: Performance figures for PMSM as a function of δ with variable flux (only design values)

Range of δ for flux variable	Achieved values				
($-8°$ to $30°$)	ϕ	cos ϕ	i_{qs}	i_{ds}	i_{phase}
$-8°$ (max. lag)	48.00	-0.55	1.92	2.9	3.48
$6.67°$ (FOC)	6.66	0.93	2.1	0.0	2.1
$8.1°$ (min. lag)	1.80	-0.24	2.1	-0.24	2.11
$8.67°$ (upf)	0.0	1.00	2.1	-0.32	2.12
$8.68°$ (min. lead)	-0.03	0.99	2.1	-0.32	2.12
$30°$ (max. lead)	-24.7	0.90	2.3	-3.25	3.98

and hence works at leading p.f. Finally the working range of motor is restricted only from $\delta = -8°$ to $30°$ from the simulation even though the range of $\delta = 0°$ to $91°$ in design guidelines.

8 Conclusion

In this paper a generalized approach to the design for the torque angle control of a non-linear vector controller of PMSM has been presented. It is found that, by the variation of torque angle (δ) there is a wide range of dynamic performance. This also gives rise to the flexibility of choosing the power factor from lagging to leading (or vice versa) through unity. The special case of Field orientation control which is obtained from a different perspective, by choosing torque angle (δ) such that the internal power factor angle (ψ) made to be zero. This result in complete decoupling between the armature and field flux, allowing them to be controlled independently, like a DC motor, improving the dynamic performance of the system.

Appendix: ratings and parameters of PMSM

Ratings of Permanent Magnet Synchronous Motor: Rated voltage $= 400$ V, Rated current $= 2.17$ A, Rated speed $= 1500$ rpm, No. of poles $= 4$, Rated Power: 1.2/1.5 kW, 0.8/1.0 p.f , $J = 0.048$ kg·m^2, $\beta = 0.0048$ N.m/ rad/sec.

Performing various tests in the laboratory, parameters of the PMSM is found as: $r_a = 6.1\Omega$, $r_{dr} = 16.0\Omega$, $r_{qr} = 4.167\Omega$, $r_{fr} = 0.3096\Omega$, $l_l = 0.016393$ H, $l_{ad} = 0.06228$ H, $l_{aq} = 0.03975$ H, $l_{fr} = 0.09227$ H, $l_{dr} = 0.14454$ H, $l_{qr} = 0.14$ H, $J = 0.048$ kg·m^2, $\beta = 0.0048$ N.m/ rad/sec.

References

[1] G. Clos. Torque angle control of the permanent magnet synchronous machine at the voltage margin. **in:** *European Conference on Power Electronics and Applications*, 2013, 1–9.

[2] U. Hasirci, A. Balikci. Nonlinear and adaptive state feedback control of variable speed PMSM drives. **in:** *Asian Control Conference, 2009. Ascc 2009.*, 2009, 1605–1610.

[3] F. Heydari, A. Sheikholeslami, et al. Predictive field-oriented control of pmsm with space vector modulation technique,. *Front. Electrical Electronics Engineering, China*, 2010, **5**(1): 91–99.

[4] M. Kadjoudj, M. E. H. Benbouzid, et al. A robust hybrid current control for permanent-magnet synchronous motor drive. *IEEE Transactions on Energy Conversion*, 2004, **19**(1): 109–115.

[5] R. Krishnan. Electric motor drives: Modeling, analysis, and control. *Prentice Hall*, 2001.

[6] G. Kron. Generalized theory of electrical machinery. *Transactions of the American Institute of Electrical Engineers*, 1930, **49**(2): 666–683.

[7] K. A. Mary, A. Patra, et al. Design and implementation of the control system for an inverter-fed synchronous motor drive. *IEEE Transactions on Control Systems Technology*, 2002, **10**(6): 853–859.

[8] P. Pillay, R. Krishnan. Modeling of permanent magnet motor drives. *IEEE Transactions on Industrial Electronics*, 1988, **35**(4): 537–541.

[9] P. Pillay, R. Krishnan. Modeling, simulation and analysis of Permanent magnet motor drives, Part-I: The permanent magnet synchronous motor drive. *IEEE Transactions on Industry Applications*, 1989, **25**(2): 265–273.

[10] P. Ramana, K. A. Mary, et al. Design methodology for field orientation control of a non-linear vector controlled sinusoidal permanent magnet ac motor. *ARPN Journal Engineering and Technology*, 2015, **10**(5): 2159–2166.

[11] P. Ramana, M. S. Kalavathi, et al. Design methodology for torque angle control of a non-linear vector controlled variable reluctance synchronous motor. **in:** *International Conference on Electrical, Electronics, Signals, Communication and Optimization*, 2015, pp 1–6.

[12] P. Ramana, B. S. Kumar, et al. Comparison of various pwm techniques for field oriented control VSI fed PMSM drive. *International Journal of Advanced Research in Electrical Electronics & Instrumentation Engineering*, 2013, **2**(7): 2928–2936.

[13] P. Ramana, K. A. Mary, et al. Design methodology for internal angle control of non-linear vector controlled variable reluctance synchronous motor. *International Journal of Applied Engineering Research*, 2015, **10**(1): 217–223.

[14] J. Zhou, Y. Wang. Adaptive backstepping speed controller design for a permanent magnet synchronous motor. *Electric Power Applications, IEE Proceedings*, 2002, **149**(2): 165–172.